

# Solvothermal Synthesis of CdS Nanowires in a Mixed Solvent of Ethylenediamine and Dodecanethiol

Dan Xu, Zhaoping Liu, Jianbo Liang, and Yitai Qian\*

Department of Chemistry, University of Science and Technology of China, Hefei, Anhui 230026, People's Republic of China

Received: April 16, 2005; In Final Form: June 3, 2005

CdS nanowires with an average diameter of 25 nm and lengths of 20–40  $\mu\text{m}$  have been solvothermally synthesized in a mixed solvent of ethylenediamine and dodecanethiol at 180  $^{\circ}\text{C}$ . The time-dependent examinations reveal that the formation process of CdS nanowires involves two sequential processes: a short-period solid–solid transformation process in the initial stage and a long-period Ostwald ripening process. The effect of both the volume ratios between the two components of the solvent and the reaction temperatures on the nanowire growth has also been investigated in detail. The results of the photoluminescence and UV–vis spectroscopy measurements reveal that the as-prepared CdS nanowires show a quantum confinement effect.

## Introduction

The fabrication of semiconducting metal chalcogenide nanowires has attracted intense interest in the past several years because of their unusual optical and electric properties and potential applications in nanodevices.<sup>1</sup> Among these metal chalcogenides, CdS has been one of the most studied due to its extensive applications in photoelectric conversion in solar cells and light-emitting diodes in flat panel displays.<sup>2</sup> CdS nanowires have been synthesized by several techniques. For instance, the growth of thin CdS nanowires ( $\sim 20$  nm thick) has been achieved by a laser ablation technique or chemical vapor deposition (CVD) process based on a gold nanocluster catalyzed vapor–liquid–solid (VLS) growth mechanism.<sup>3</sup> CdS nanowires with diameters of 30–70 nm have also been synthesized simply by thermal evaporation of CdS powders.<sup>4</sup> Nevertheless, the above-mentioned methods need some special instruments, harsh conditions, and/or relatively high performance temperature (over 800  $^{\circ}\text{C}$ ). Uniform nanowires of CdS could also be obtained in the channels of various templates, such as anodic aluminum oxide (AAO) membrane,<sup>5</sup> polymer gels,<sup>6</sup> micelles,<sup>7</sup> and so on.<sup>8</sup> Although the template-directed methods are effective in preparing nanowires with uniform and controllable dimensions, they usually lead to a complicated process and also impurities due to the incomplete removal of the templates, and the yields are relatively low. Moreover, CdS nanowires have also been prepared by a solvothermal process,<sup>9</sup> which may provide a more promising technique for preparing CdS nanowires than conventional methods in terms of cost and potential for large-scale production. Our group reported that CdS nanowires/nanorods could be obtained in the coordinating solvent ethylenediamine via a solvothermal reaction or directly via a solvothermal recrystallization process;<sup>9a–e</sup> Zhao and co-workers further found that CdS nanowires with a length of up to 3  $\mu\text{m}$  could be produced by adding the ligand 8-hydroxyquinoline to the reaction system (a so-called ligand-assisted solvothermal process).<sup>9f</sup> However, these synthesized CdS nanowires were still

unsatisfactory in their lengths (at most several micrometers). Hence, it should be very interesting and important to further develop an effective solvothermal process for the synthesis of CdS nanowires with a considerable length and a high aspect ratio. Some of our recent studies have shown that the use of mixed solvents in some cases has a clear advantage for the fabrication of ultralong nanowires or nanoribbons of metal sulfides.<sup>10</sup> In this paper, we demonstrate that high-quality CdS nanowires ( $\sim 25$  nm in diameter; 20–40  $\mu\text{m}$  in length; aspect ratio over 1000) can be solvothermally synthesized in a large scale in a mixed solvent of ethylenediamine and dodecanethiol.

## Experimental Section

**Synthesis.** All of the chemical reagents used in this experiment were of analytical grade and used without further purification. Cadmium acetate ( $\text{Cd}(\text{OAc})_2 \cdot 2\text{H}_2\text{O}$ ), sodium bis(diethyldithiocarbamate) ( $\text{NaS}_2\text{CNET}_2 \cdot 3\text{H}_2\text{O}$ ), ethylenediamine ( $\text{C}_2\text{N}_2\text{H}_8$ ), and dodecanethiol ( $\text{C}_{12}\text{H}_{25}\text{SH}$ ) were purchased from Shanghai Chemical Reagents Company. In a typical procedure, 1 mmol of  $\text{Cd}(\text{OAc})_2 \cdot 2\text{H}_2\text{O}$  and 2 mmol of  $\text{NaS}_2\text{CNET}_2 \cdot 3\text{H}_2\text{O}$  were introduced into a mixed solvent of ethylenediamine and dodecanethiol (with volume of 17 and 3  $\text{cm}^3$ , respectively). After 5 min of stirring, the resulting reaction mixture was transferred into a Teflon-lined stainless autoclave (25  $\text{cm}^3$  capacity). The autoclave was sealed and maintained in an electric oven at 180  $^{\circ}\text{C}$  for 48 h, and then cooled to room temperature naturally. The product was carefully collected and washed with distilled water and absolute ethanol several times, and then dried in a vacuum at 50  $^{\circ}\text{C}$  for 4 h.

**Characterization.** X-ray diffraction (XRD) analysis was performed using a Philip X'Pert PRO SUPER  $\gamma$ A rotation anode with Ni-filtered Cu K $\alpha$  radiation ( $\lambda = 1.54178$  Å). Field emission scanning electron microscopic (FESEM) images were taken on a JEOL JSM-6700F SEM. The transmission electron microscopic (TEM) images and selected-area electron diffraction (SAED) patterns were recorded on a Hitachi Model H-800 instrument at an accelerating voltage of 200 kV. High-resolution TEM images were performed with a JEOL-2010 TEM at an acceleration voltage of 200 kV. Fourier transform infrared

\* To whom correspondence should be addressed. Phone: +86-551-3603204. Fax: +86-551-3607402. E-mail: yitaiqian@ustc.edu.cn.

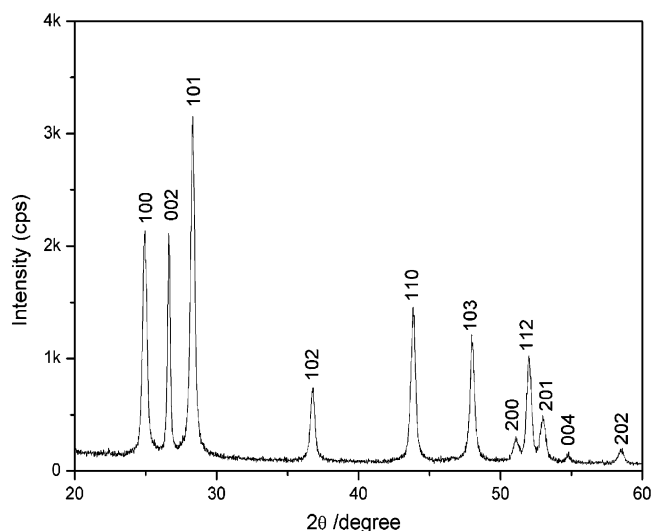


**Figure 1.** XRD pattern of the product.

(FTIR) absorption spectra were obtained with a Shimadzu IR-440 spectrometer. Thermogravimetric (TG) measurement of the sample was conducted on a Shimadzu TGA-50H analyzer. UV-vis absorption spectra were recorded on a Shimadzu UV-vis spectrophotometer (UV-240). Photoluminescence (PL) measurements were carried out on a Perkin-Elmer LS-55 luminescence spectrometer using a pulsed Xe lamp.

## Results and Discussion

**Structure and Morphology.** Figure 1 shows a typical XRD pattern of the as-synthesized product. All the diffraction peaks can be readily indexed as wurtzite CdS with lattice constants  $a = 4.139 \text{ \AA}$  and  $c = 6.720 \text{ \AA}$ , in good agreement with the literature values (JCPDS Card No. 41-1049). No peaks of impurities were detected, indicating the high purity of the product. In addition, the intense and sharp diffraction peaks suggest the obtained product is well crystallized.

The morphology and dimension of the product were examined by FESEM. Typical FESEM images of the product are shown in Figure 2. As can be seen, the product is composed of uniform nanowires with an average diameter of 25 nm and lengths in the range of 20–40  $\mu\text{m}$ . These images demonstrate that CdS nanowires with a small thickness and a high aspect ratio can be readily prepared on a large scale by the present method. The microstructure of individual CdS nanowires was investigated in detail by HRTEM and SAED. Figure 3a shows a representa-

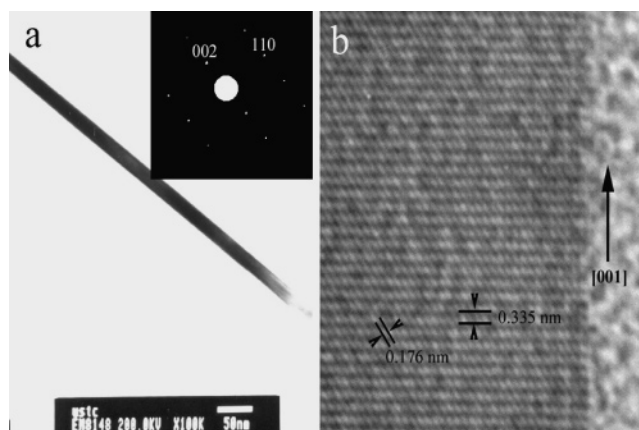


**Figure 3.** (a) Typical TEM image of a single CdS nanowire. The inset is a SAED pattern taken along the  $[1\bar{1}0]$  zone axis direction. (b) HRTEM image taken from the edge of the nanowire shown in (a).

tive TEM image of a single nanowire with a thickness of  $\sim 20$  nm. The inset SAED pattern of this nanowire was recorded with the electron beam along the  $[1\bar{1}0]$  zone axis of wurtzite CdS. The corresponding HRTEM image (Figure 3b) shows two sets of regular lattice fringes of ca. 0.335 and 0.176 nm that are consistent with the (002) and (112) crystal planes of the wurtzite CdS, respectively. Both the HRTEM image and SAED pattern reveal that the as-prepared CdS nanowires are of single crystals with a preferential growth direction of  $[001]$ ,  $c$ -axis.

**Formation Process of Nanowires.** To understand the formation mechanism of CdS nanowires, we have systematically investigated the samples obtained at different stages of the reaction using the TEM and XRD techniques. Figure 4 shows the TEM images of the samples obtained after the reaction proceeded for 30 min, 45 min, 2 h, and 4 h, respectively. These images clearly show the transformation process of the particle morphologies from spherical to clewlike, to rodlike, and finally to wirelike. When the reaction proceeded for 30 min, the sample was composed mainly of quasi-spherical particles with sizes in the range of 20–100 nm, as shown in Figure 4a. These particles were viscous to some extent and were aggregated. Focusing the electronic beam on such particles did not produce any electron diffraction pattern (see the inset in Figure 4a), suggesting that they may be amorphous. The XRD pattern (Figure 5a) of this sample shows many reflections in high angles ( $2\theta$  10–70°), but these reflections cannot be indexed to any known inorganic phases. However, the low-angle XRD pattern (see the inset of Figure 5) shows a series of basal reflections with  $d(001) = 3.36$

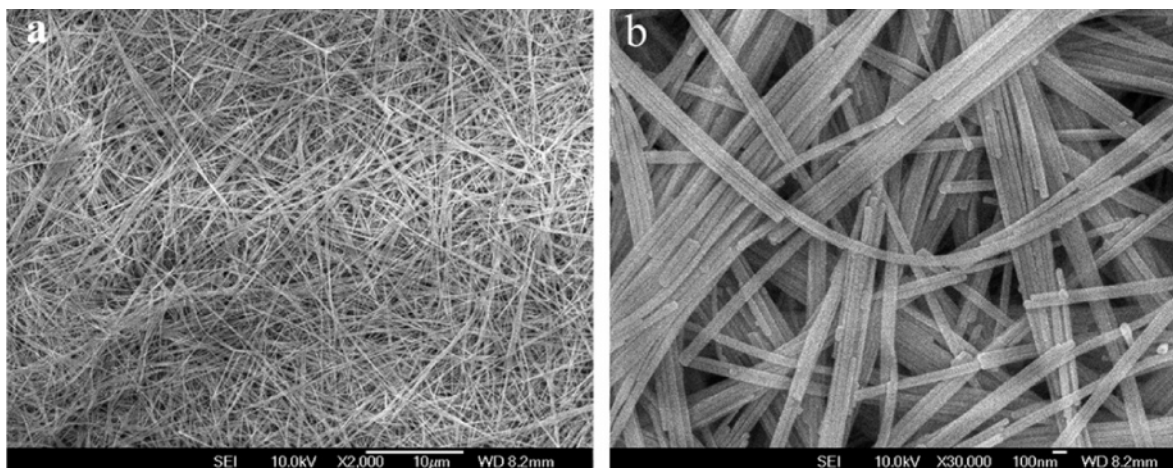


**Figure 2.** (a) Low- and (b) high-magnification FESEM images of the product.

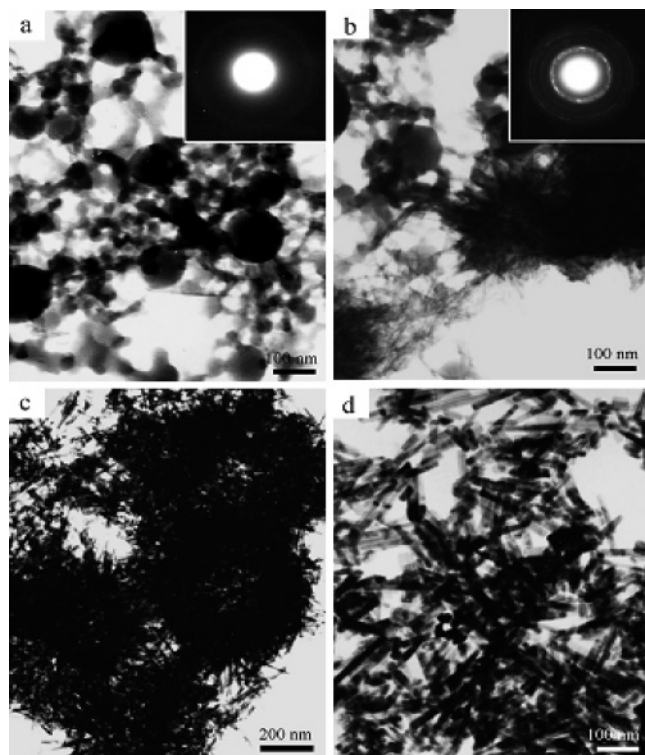


**Figure 4.** TEM images of four samples, showing different growth stages of CdS nanocrystals. These samples were taken after different aging times: (a) 30 min, (b) 45 min, (c) 2 h, and (d) 4 h. Insets in (a) and (b) show the corresponding ED patterns.

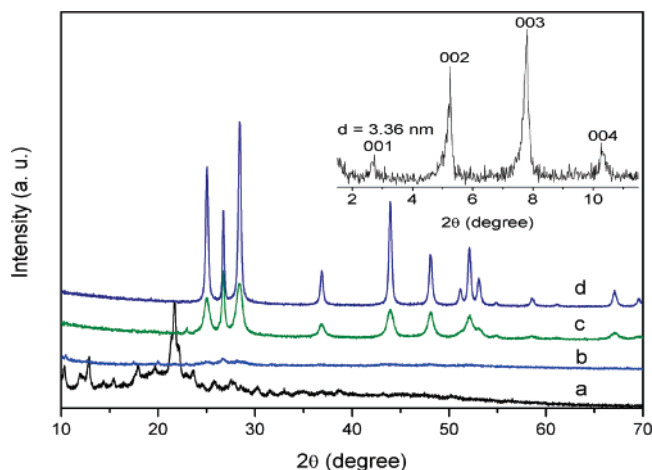


**Figure 5.** XRD patterns of samples obtained at different growth stages: (a) 30 min, (b) 45 min, (c) 2 h, and (d) 4 h.

nm, indicative of a layered structure. Taking into consideration that dodecanethiol molecules have a length of about 1.7 nm,<sup>11</sup> it can thus be believed that a layered phase of  $\text{Cd}(\text{SC}_{12}\text{H}_{25})_2$  formed with a layer spacing that approximately equaled the length of double dodecanethiol molecules. Evidence for the presence of  $\text{Cd}(\text{SC}_{12}\text{H}_{25})_2$  can be found in FTIR spectra (Figure 6). The similarity between the FTIR spectrum (curve a of Figure 6) of the 30-min product to that (curve b of Figure 6) of the free dodecanethiol indicates that the initial product contains  $\text{Cd}(\text{SC}_{12}\text{H}_{25})_2$ ; moreover, curve a does not show the absorption band at about  $2577\text{ cm}^{-1}$  that is characteristic of the S–H group of free dodecanethiol molecules, further confirming that the product is a thiolate indeed.<sup>12</sup> This compound was precipitated initially via a reaction between cadmium salts and dodecanethiol. Nevertheless, under the solvothermal conditions, the reaction between  $\text{Cd}(\text{SC}_{12}\text{H}_{25})_2$  and the sulfur source ( $\text{NaS}_2\text{CNET}_2$ ) would

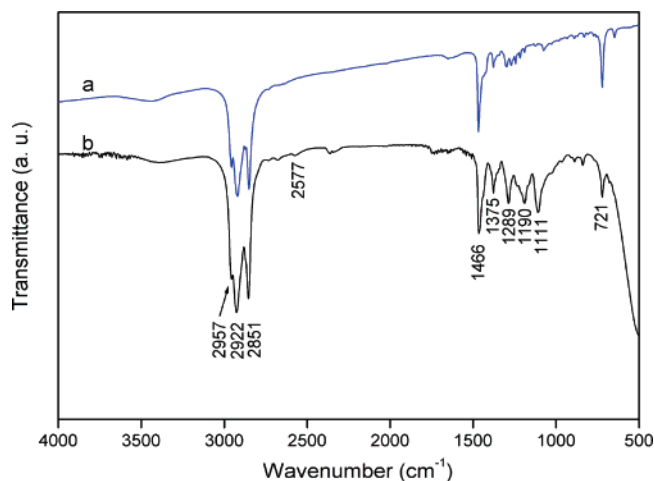


**Figure 6.** FTIR spectra of 30-min product (curve a) and free dodecanethiol (curve b). The spectrum of free dodecanethiol has been well indexed in the literature.<sup>12</sup> Three well-resolved peaks at 2851, 2922, and  $2957\text{ cm}^{-1}$  are assigned to methylene C–H symmetric, methylene C–H antisymmetric, and methyl asymmetric vibrational absorption bands. The weak absorption peak at  $2577\text{ cm}^{-1}$  is attributed to the S–H stretching band. The sharp peak at  $1466\text{ cm}^{-1}$  corresponds to the methylene scissoring mode. The peak at  $1375\text{ cm}^{-1}$  is assigned to the symmetric bending vibration of methyl group. The bands between 1100 and  $1300\text{ cm}^{-1}$  are attributed to the wag–twist progression mode of conformationally ordered chains. The peak at  $721\text{ cm}^{-1}$  is due to the methylene rocking.

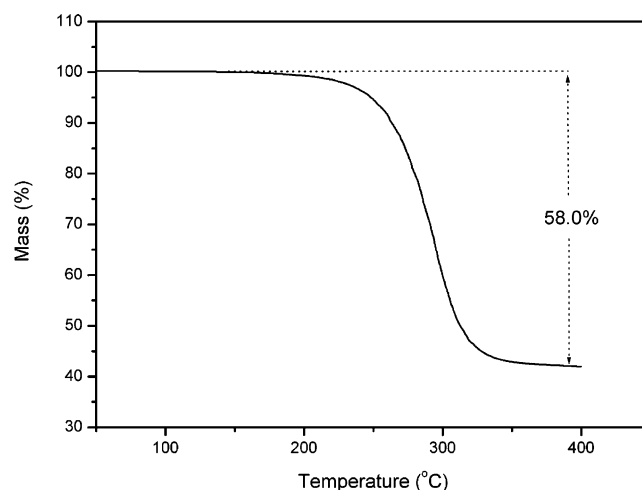


**Figure 7.** TG curve of the 30-min product.

occur immediately and generate some intermediates such as  $\text{Cd}(\text{SC}_{12}\text{H}_{25})(\text{NaS}_2\text{CNET}_2)$  and  $\text{Cd}(\text{S}_2\text{CNET}_2)_2$ .<sup>13</sup>

The TG curve (Figure 7) shows that the 30-min product undergoes a single-step weight loss (58.0%), which is between the net weight loss (ca. 71.9%) of pure  $\text{Cd}(\text{SC}_{12}\text{H}_{25})_2$  and that (ca. 47.4%) of  $\text{Cd}(\text{S}_2\text{CNET}_2)_2$ . This result indicates that the 30-min product may be a mixture of the above-mentioned intermediates. As the reaction proceeded, more  $\text{Cd}(\text{S}_2\text{CNET}_2)_2$  might be formed, and then it decomposed rapidly into CdS. As shown in Figure 5b, the XRD pattern of the 45-min product displays only the reflections of wurtzite CdS. These reflections are much weaker and broader, indicating that the CdS product is poorly crystallized. A TEM image (Figure 4b) of this sample shows that a thick layer of short nanowhiskers with a extremely small diameter ( $\sim 2\text{ nm}$ ) has grown on the surfaces of most of spherical particles. The particles thus look like clews. The SAED pattern (inset of Figure 4b) taken from a clewlike particle shows several weak diffraction rings of wurtzite CdS, verifying their poor crystallinity. As the reaction proceeded for 2 h, it was found



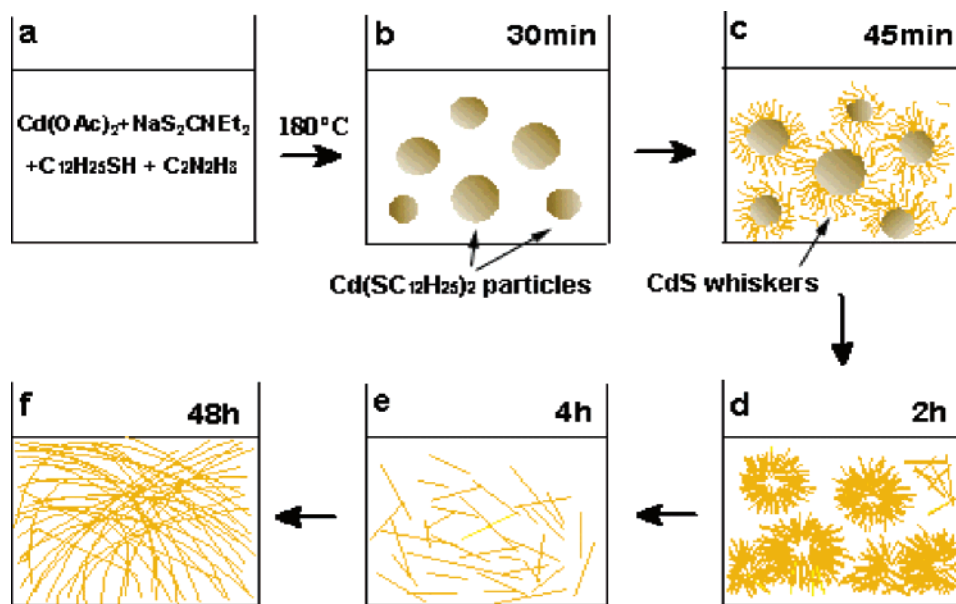


**Figure 8.** Schematic illustration of the formation process of CdS nanowires, which can be rationally supported by TEM studies given in Figure 4.

that most of the clews transformed to hollow clews and at the same time the nanowhiskers grown on their surfaces became thicker ( $\sim 5$  nm); it was also observed that some nanowhiskers had broken away from the parent clews (see Figure 4c). The corresponding XRD pattern (Figure 5c) reveals a significant increase in the crystallinity. After aging for 4 h, all the hollow clews had broken completely and thus the product was composed of short nanorods and nanoparticles (see Figure 4d). These nanorods have a much increased thickness ( $\sim 20$  nm) but have little changed length compared with the nanowhiskers. The XRD pattern (Figure 5d) indicates that the sample has a further increased crystallinity. Further extending the aging time, these nanorods were found to develop into long nanowires gradually. As illustrated in Figure 2, the 48-h product is dominated by CdS nanowires with a much increased length (20–40  $\mu\text{m}$ ). However, the as-grown nanowires have a slightly increased average thickness (25 nm) in comparison with that (20 nm) of the pristine nanorod.

The above investigations suggest that the formation of CdS nanowires undergoes four distinctive stages: (1) the formation of spherical particles through the solvothermal reactions between  $\text{Cd}(\text{OAc})_2$ ,  $\text{C}_{12}\text{H}_{25}\text{SH}$ , and  $\text{NaS}_2\text{CNEt}_2$ ; (2) the growth of thin nanowhiskers of CdS on the surfaces of the spherical particles, resulting in the formation of clewlike particles; (3) the growth of thicker nanorods based on nanowhiskers and the subsequent rupture of clewlike particles into polydispersed nanorods; (4) the evolution of long nanowires. Such a formation process of CdS nanowires is depicted schematically in Figure 8. The first three stages are involved in a solid–solid transformation process from  $\text{Cd}(\text{SC}_{12}\text{H}_{25})_2$  to  $\text{Cd}(\text{S}_2\text{CNEt}_2)_2$ , and finally to CdS, while the last stage is a Ostwald ripening process as described elsewhere.<sup>14</sup> The former process was performed in a relative short period of the reaction time ( $\sim 4$  h), and the latter ripening process took a period as long as 2 days.

**Solvent Effect.** In the previous work of our group, the synthesis of CdS one-dimensional (1D) nanostructures was achieved by a solvothermal process using ethylenediamine as the solvent,<sup>9a–c</sup> and especially CdS nanorods were formed directly from CdS nanoparticles in ethylenediamine via a solvothermal recrystallization process.<sup>9e</sup> The growth of CdS 1D nanostructures in ethylenediamine was attributed to the highly

anisotropic crystal structure and also the structure-directing coordination template effect of ethylenediamine. Recently, Zhao's group reported that multiarmed CdS nanorods could be solvothermally prepared in ethylenediamine and dodecanethiol containing toluene solution; they also believed that both ethylenediamine and dodecanethiol might serve as the structure-directing agents for the nanorod growth.<sup>9d</sup> In the present study, the use of the mixture of ethylenediamine and dodecanethiol as the reaction medium has resulted in the growth of long nanowires with lengths of up to tens of micrometers. To better understand the exact roles of the components of the solvent, we have investigated in detail the effect of their relative volumes on the size of the produced particles.

When dodecanethiol was used alone as the solvent, the product was composed of irregular nanoparticles (see Figure 9a), indicating that 1D growth of CdS could not occur in a dodecanethiol medium. The control experiments have revealed that CdS nanowires with a uniform thickness and a high aspect ratio could be obtained with a volume of dodecanethiol between 1 and 5  $\text{cm}^3$  (the total volume of solvent was fixed at 20  $\text{cm}^3$ ). With a volume of dodecanethiol more than 5  $\text{cm}^3$ , the produced 1D nanostructures became shorter and thicker; and no nanowires could be obtained when the volume of dodecanethiol was greater than 10  $\text{cm}^3$  (half of the total volume). Parts b and c of Figure 9 show the TEM images of the products that were prepared with 10 and 15  $\text{cm}^3$  of dodecanethiol, respectively. As can be seen, these products are composed of short and thick nanorods with nonuniform lengths of hundreds of nanometers. On the other hand, a too-small amount of dodecanethiol resulted in the formation of short nanowires or nanorods. For example, the product prepared with 0.2  $\text{cm}^3$  of dodecanethiol was composed of nanorods with lengths of less than 2  $\mu\text{m}$  (see Figure 9d). The above results suggest that both ethylenediamine and dodecanethiol play important roles on the growth of CdS nanowires. Owing to the presence of dodecanethiol, the CdS nanorods and nanoparticles were formed at the beginning via a solid–solid transformation process (from  $\text{Cd}(\text{SC}_{12}\text{H}_{25})_2$  to  $\text{Cd}(\text{S}_2\text{CNEt}_2)_2$ , and finally to CdS) as described earlier. The FTIR studies revealed that this process was not involved in any ethylenediamine-containing intermediates such as  $\text{CdS}\cdot 0.5\text{en}$  (en stands for ethylenediamine) as reported elsewhere.<sup>15</sup> Due to the

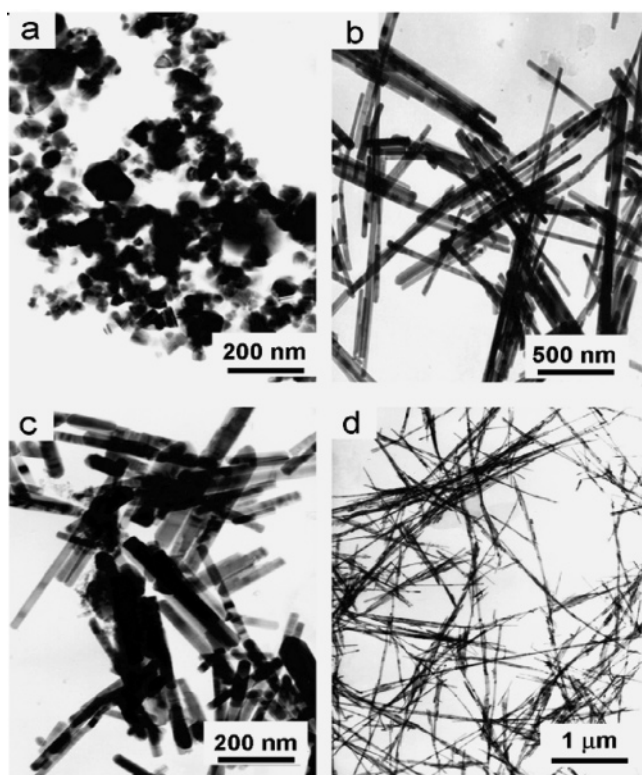


**Figure 9.** TEM images of products prepared with different volumes of dodecanethiol: (a) 20, (b) 10, (c) 15, and (d) 0.2 cm<sup>3</sup>. Note that the total volume of the solvent used was fixed at 20 cm<sup>3</sup>.

strong coordination ability of ethylenediamine, part of the CdS nanocrystals with smaller sizes, which had high free energies, were gradually dissolved and got into the solution phase through the formation of a complex of Cd<sup>2+</sup> and ethylenediamine, Cd(en)<sub>2</sub><sup>2+</sup>, and then the dissolved Cd and S species spontaneously would transfer and recrystallize onto the surfaces (usually {001} planes) of large-size nanorods with high surface free energies. At the expense of these small nanoparticles, nanorods would grow continuously into long nanowires via an Ostwald ripening process. As described in the literatures,<sup>9</sup> ethylenediamine molecules also acted as the capping ligands that selectively adsorbed onto the lateral surfaces of the 1D nanostructures. As a result, the lateral growth of nanowires was restrained largely, as supported by the TEM observations. Thus, ethylenediamine mainly served as the coordination solvent as well as the capping ligand, which played a crucial role in the dissolution of small particles and the 1D growth of large nanorods.

**Temperature Effect.** It was found that the solvothermal temperature was also a key factor that influenced the particle size. At a temperature as low as 150 °C, the reaction only gave short nanorods with a size of ~20 nm × 200 nm (see Figure 10a), indicating that the 1D growth of CdS nanocrystals proceeded at a very slow rate and thus a relatively longer period of the ripening process was needed for the evolution of long nanowires. Elevating the temperature could accelerate the 1D growth of CdS nanocrystals and lead to the formation of long nanowires. At an too-high temperature, however, the adsorption of the capping ligands (ethylenediamine molecules) on the lateral surfaces of the growing 1D nanocrystals might be much weakened, and thus the 1D nanocrystals have a relatively faster lateral growth rate, resulting in the formation of thicker nanowires or nanorods. As depicted in Figure 10b, the product obtained at 200 °C was much thicker nanorods with thicknesses

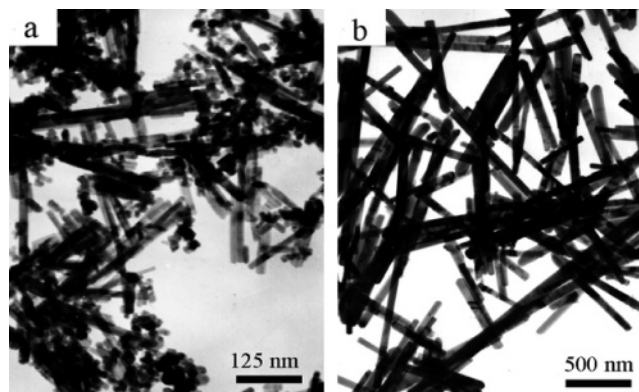


**Figure 10.** TEM images of products obtained at different temperatures: (a) 150 and (b) 200 °C.

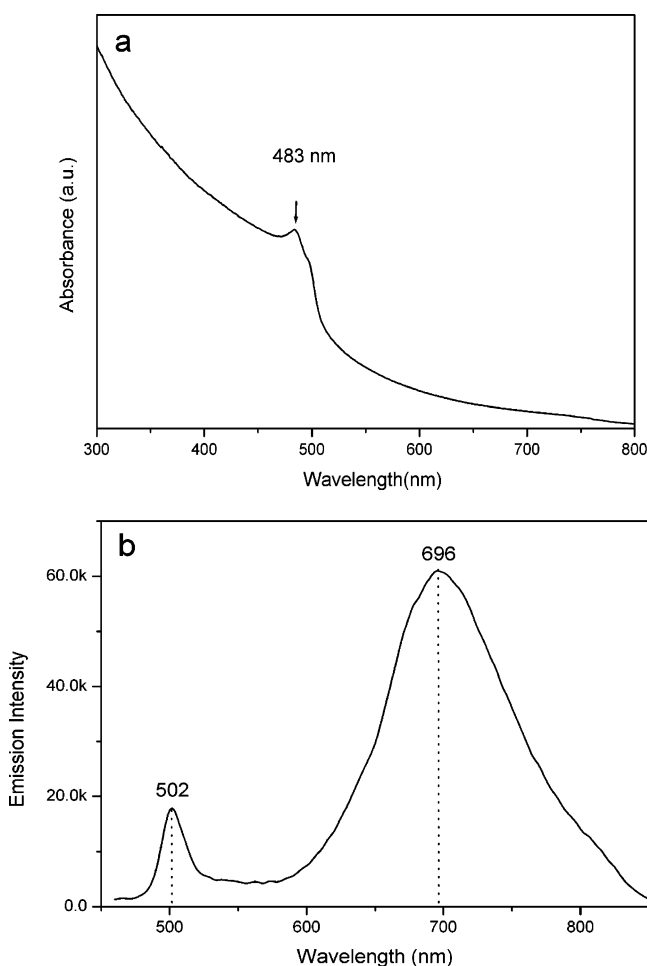


**Figure 11.** UV-vis absorption spectrum (a) and photoluminescence spectrum (b) of as-prepared CdS nanowires with 25 nm mean diameter and 20–40 μm lengths.

in the range of 50–100 nm and lengths of only hundreds of nanometers. The experimental results revealed that the solvothermal temperatures ranging from 160 to 180 °C were optimum for the formation of thin and long nanowires.

**Optical Properties.** We also carried out some basal optical property examinations to evaluate the quality of the product. Figure 11a shows the UV-vis spectrum of the as-prepared CdS nanowires (25 nm thick and 20–40 μm long). The absorption peak appears at 483 nm, and it is blue-shifted compared with that of bulk CdS (513 nm),<sup>16</sup> indicating the presence of the quantum size effect. The room-temperature PL spectrum of the same sample is shown in Figure 11b. It displays two distinct

emission bands that are a green emission band at 502 nm (2.47 eV) and an infrared band at 696 nm (1.78 eV), which are close to those in previous reports for CdS nanocrystals.<sup>17</sup> The former emission band can be assigned to near-band-edge emission, and the latter one is associated with structural defects, which may arise from the excess of sulfur or core defects on the nanowire surfaces.<sup>18</sup>

## Conclusion

In summary, uniform and high aspect ratio CdS nanowires have been synthesized successfully on a large scale by a solvothermal process in a mixed solvent of dodecanethiol and ethylenediamine. The formation of CdS nanowires undergoes four morphological changes from spherical particles to clewlike structures, to nanorods, and finally to nanowires, and these changes involve a short-period solid–solid transformation process and then a long-period ripening process. By carefully adjusting the volume ratios of both components of the solvent or the solvothermal temperatures, CdS nanorods and nanowires with different dimensions can be controllably synthesized. The present synthetic scheme is proven to be effective for the preparation of CdS nanowires with high aspect ratios, and it may be extended to the synthesis of other chalcogenide nanowires by selecting some appropriate metal and/or chalcogen sources.

**Acknowledgment.** This work was supported by the National Natural Science Foundation of China and the 973 Project of China.

## References and Notes

- (1) (a) Xia, Y. N.; Yang, P. D.; Sun, Y. G.; Wu, Y. Y.; Mayers, B.; Gates, B.; Yin, Y. D.; Kim, F.; Yan, H. Q. *Adv. Mater.* **2003**, *15*, 353. (b) Rao, C. N.; Deepak, F. L.; Gundiah, G.; Govindaraj, A. *Prog. Solid State Chem.* **2003**, *31*, 5–147. (c) Golden, J. H.; DiSalvo, F. J.; Frechet, J. M. J.; Silcox, J.; Thomas, M.; Elman, J. *Science* **1996**, *273*, 782. (d) Prieto, A. L.; Sander, M. S.; Martin-Gonzalez, M. S.; Gronsky, R.; Sands, T.; Stacy, A. M. *J. Am. Chem. Soc.* **2001**, *123*, 7160.
- (2) (a) Morkel, M.; Weinhardt, L.; Lohmüller, B.; Heske, C.; Umbach, E.; Riedl, W.; Zweigart, S.; Karg, F. *Appl. Phys. Lett.* **2001**, *79*, 4482. (b) Schlamp, M. C.; Peng, X. G.; Alivisatos, A. P. *J. Appl. Phys.* **1997**, *82*, 5837.
- (3) (a) Duan, X. F.; Lieber, C. M. *Adv. Mater.* **2000**, *12*, 298. (b) Barrelet, C. J.; Wu, Y.; Bell, D. C.; Lieber, C. M. *J. Am. Chem. Soc.* **2003**, *125*, 11498.
- (4) (a) Ye, C.; Meng, G.; Wang, Y.; Jiang, Z.; Zhang, L. *J. Phys. Chem. B* **2002**, *106*, 10338. (b) Wang, Y.; Meng, G.; Zhang, L.; Liang, C.; Zhang, J. *Chem. Mater.* **2002**, *14*, 1773.
- (5) (a) Routkevitch, D.; Bigioni, T.; Moskovits, M.; Xu, J. M. *J. Phys. Chem.* **1996**, *100*, 14037. (b) Xu, D. S.; Xu, Y. J.; Chen, D. P.; Guo, G. L.; Gui, L. L.; Tang, Y. Q. *Adv. Mater.* **2000**, *12*, 520.
- (6) Zhan, J.; Yang, X.; Wang, D.; Li, S.; Xie, Y.; Xia, Y. N.; Qian, Y. T. *Adv. Mater.* **2000**, *12*, 1348.
- (7) Xiong, Y. J.; Xie, Y.; Yang, J.; Zhang, R.; Wu, C. Z.; Du, G. A. *J. Mater. Chem.* **2002**, *12*, 3712.
- (8) (a) Gao, F.; Lu, Q. Y.; Zhao, D. Y. *Adv. Mater.* **2003**, *15*, 739. (b) Zhang, X. J.; Xie, Y.; Zhao, Q. R.; Tian, Y. P. *New J. Chem.* **2003**, *27*, 827.
- (9) (a) Li, Y. D.; Liao, H. W.; Ding, Y.; Fan, Y.; Zhang, Y.; Qian, Y. T. *Inorg. Chem.* **1999**, *38*, 1382. (b) Yu, S. H.; Wu, Y. S.; Yang, J.; Han, Z. H.; Xie, Y.; Qian, Y. T.; Liu, X. M. *Chem. Mater.* **1998**, *10*, 2309. (c) Yang, J.; Zeng, J. H.; Yu, S. H.; Yang, L.; Zhou, G. E.; Qian, Y. T. *Chem. Mater.* **2000**, *12*, 3259. (d) Gao, F.; Lu, Q. Y.; Xie, S. H.; Zhao, D. Y. *Adv. Mater.* **2002**, *14*, 1537. (e) Chen, M.; Xie, Y.; Lu, J.; Xiong, Y. J.; Zhang, S. Y.; Qian, Y. T.; Liu, X. M. *J. Mater. Chem.* **2002**, *12*, 748. (f) Gao, F.; Lu, Q. Y.; Zhao, D. Y. *Chem. Lett.* **2002**, *7*, 732.
- (10) (a) Liu, Z. P.; Peng, S.; Xie, Q.; Hu, Z. K.; Yang, Y.; Zhang, S. Y.; Qian, Y. T. *Adv. Mater.* **2003**, *15*, 936. (b) Liu, Z. P.; Xu, D.; Liang, J. B.; Shen, J. M.; Zhang, S. Y.; Qian, Y. T. *J. Phys. Chem. B* **2005**, *109*, 10699.
- (11) Motte, L.; Billoudet, F.; Pileni, M. P. *J. Phys. Chem.* **1995**, *99*, 16425.
- (12) (a) Aslam, M.; Mulla, I. S.; Vijayamohan, K. *Langmuir* **2001**, *17*, 7487. (b) Yee, C. K.; Ulman, A.; Ruiz, J. D.; Parikh, A.; White, H.; Rafailovich, M. *Langmuir* **2003**, *19*, 9450. (c) Ang, T. P.; Wee, T. S. A.; Chin, W. S. *J. Phys. Chem. B* **2004**, *108*, 11001. (d) Chaki, N. K.; Vijayamohan, K. *J. Phys. Chem. B* **2005**, *109*, 2552.
- (13) (a) Yan, P.; Xie, Y.; Qian, Y. T.; Liu, X. M. *Chem. Commun.* **1999**, *14*, 1293. (b) Lu, J.; Xie, Y.; Du, G. A.; Jiang, X. C.; Zhu, L. Y.; Wang, X. J.; Qian, Y. T. *J. Mater. Chem.* **2002**, *12*, 103.
- (14) (a) Talapin, D. V.; Rogach, A. L.; Haase, M.; Weller, H. *J. Phys. Chem. B* **2001**, *105*, 12278. (b) Min, B. D.; Kim, Y.; Kim, E. K.; Min, S. K.; Park, M. *J. Phys. Rev. B* **1998**, *57*, 11879. (c) Sun, Y. G.; Mayers, B.; Herricks, T.; Xia, Y. N. *Nano Lett.* **2003**, *3*, 955.
- (15) Deng, Z. X.; Li, L.; Li, Y. *Inorg. Chem.* **2003**, *42*, 2331.
- (16) Weller, H. *Angew. Chem., Int. Ed. Engl.* **1993**, *32*, 41.
- (17) (a) Liu, B.; Xu, G. Q.; Gan, L. M.; Chew, C. H.; Li, W. S.; Shen, Z. X. *J. Appl. Phys.* **2001**, *89*, 1059. (b) Matsuura, D.; Kanemitsu, Y.; Kushida, T.; White, C. W.; Budai, J. D.; Meldrum, A. *Appl. Phys. Lett.* **2000**, *77*, 2289. (c) Bawendi, M. G.; Carroll, P. J.; Wilson, W. L.; Brus, L. E. *J. Chem. Phys.* **1992**, *96*, 946. (d) Ma, G.; Tang, S.; Sun, W.; Shen, Z.; Huang, W.; Shi, J. *Phys. Lett. A* **2002**, *A299*, 581. (e) Pinna, N.; Weiss, K.; Urban, J.; Pileni, M. *Adv. Mater.* **2001**, *13*, 261.
- (18) Butty, J.; Peyghambarian, N. *Appl. Phys. Lett.* **1996**, *69*, 3224.